Received: 5 March 2021 | Revised: 5 August 2021 | Accepted: 16 August 2021

DOI: 10.1002/jemt.23917

RESEARCH ARTICLE

MICROSCOPY RESEARCH & TECHNIQUE WILEY

Determination of the composition and thickness of chromel and alumel thin films on different substrates by quantitative energy dispersive spectroscopy analysis

Raissa Lima de Oblitas | Fernanda de Sá Teixeira | Maria Cecília Salvadori

Instituto de Física, Universidade de São Paulo, São Paulo, Brazil

Correspondence
Raissa Lima de Oblitas, Instituto de Física, Universidade de São Paulo, São Paulo, SP, 05508090, Brazil.
Email: raissa.oblitas@usp.br

Funding information
Conselho Nacional de Desenvolvimento Científico e Tecnológico, Grant/Award Numbers: 156484/2014-5, 302409/2018-1; Coordenação de Aperfeiçoamento de Pessoal de Nível Superior, Grant/Award Number: Finance Code 001; Fundação de Amparo à Pesquisa do Estado de São Paulo, Grant/Award Number: 2000/08231-1

Review Editor: Chuanbin Mao

Abstract

Thin films of two alloys (chromel and alumel), with thickness less than 100 nm, were obtained by plasma deposition technique, namely filtered cathodic vacuum arc (FCVA). The elemental analyses were performed by quantitative energy dispersive spectroscopy (EDS) microanalysis and Rutherford backscattering spectrometry (RBS). The applicability of EDS to such thin films as these was established by analysis of films deposited on substrates of different atomic numbers, specifically vitreous carbon, silicon, copper, and tin. We found that a substrate with atomic number similar to the mean atomic number of the film constituents is best for reliable EDS results, when compared to RBS. The compatibility between quantitative EDS measurements and RBS measurements, as well as comparison between the thin film elemental composition and the bulk material composition, was assessed by statistical analysis. Good consistency between EDS and RBS measurements was found for both chromel and alumel thin films when copper was used as substrate material. We observed severely overlapping peaks in the RBS output for the case of alumel films so that EDS analysis was crucial. We also compared thickness measurements determined by EDS and RBS, and we found good agreement for the case of alumel film on copper substrate, and 15% agreement for chromel film on copper substrate.

KEYWORDS
alumel, chromel, energy dispersive spectroscopy, quantitative microanalysis, thin films

1 | INTRODUCTION

Thin films have an extremely important role in the great advances in high-tech industry. Great exploration is in microelectronics, but thin films have a broad range of applications since they can modify or coat surfaces. Thus, the importance of techniques that are used to produce and also to characterize them has been made quite relevant.

To produce thin films, we performed filtered cathodic vacuum arc (FCVA) technique, which is often used for film deposition. In this process, the films are formed through the energetic condensation of plasma that is created from a metallic cathode in a vacuum arc plasma gun and subsequently magnetically filtered to remove cathode debris contaminants (solid particulates of cathode material). The method is appropriate for modification of surfaces and interfaces and for the synthesis of thin films of a variety of different materials and structures. Thin films of metals and alloys, ceramics, diamond-like carbon, some semiconductors, and superconductors can be produced (Anders, 2008; Brown, 1998).

The cathode of the plasma gun is typically a short cylindrical section (a short rod of 10 mm in diameter) of the material that is to be deposited, and ideally the plasma composition and also the thin film composition is the same as the composition of the cathode material. While this supposition is in general valid for simple cathodes of a single metallic element, an important question concerns how closely the

elemental composition of the film mirrors that of the cathode when a multi-element cathode is used for deposition of more complex film compositions. We note that although the deposition is performed in high vacuum ($\approx 10^{-6}$ Torr), the presence of some oxygen is inevitable, leading to incorporation of some oxygen in the film (Walkowicz, Bujak, & Zavaleyev, 2010), as well as other possible contaminants (Martins, Salvadori, Verdonck, & Brown, 2002). In the work described here, the thin film deposition was made by own bulk material, that is the multi-element cathodes used were chromel and alumel alloys, resulting in thin films with thickness less than 100 nm. The characterization of these alloys are relevant due to their thermoelectric properties being widely used for thermocouples, including thin film thermocouples (Liu, Mitsutake, & Monde, 2020; Satish et al., 2017). Chromel is an alloy composed primarily of nickel (about 90%), with some chromium. Alumel is also composed mostly of nickel (about 95%), with a variable percentage of aluminum and other elements.

In order to verify whether such thin films mirror cathode material, we used scanning electron microscopy/energy dispersive spectroscopy (SEM/EDS) and Rutherford backscattering spectrometry (RBS) to characterize the elemental composition of the chromel and alumel thin films. We also used SEM/EDS to characterize the bulk cathode material used in the vacuum arc plasma gun. The possibility of measuring the composition not only of bulk material but also of thin film samples using the EDS technique is of considerable interest due to the wide availability of the necessary instrumentation which is more economic and accessible compared to RBS technique (Kang, Limandri, Castellano, Suárez, & Trincavelli, 2017); thus, we have also established the suitability of this approach. To verify the accuracy of the thin film measurements by SEM/EDS, we adopted the RBS measurements as a reference. To assess the compatibility between measurements by EDS and RBS and between thin films and cathode material, we employed statistical techniques using Student's *t*-Test with a significance level of 5%.

Conventional quantitative SEM/EDS (Goldstein et al., 2003), although well-established for elemental compositional analysis of the homogeneous specimens in the beam interaction volume (of the order of some μm^3), is not ideal for inhomogeneous specimens. Thin film on substrate represents a case in which there is inhomogeneity in the depth dimension and, however, it does not follow the protocol of a conventional analysis, requiring the search for methods and specific corrections. SEM/EDS is part of a techniques family called electron probe microanalysis (EPMA). Correction procedures based on the use of X-ray depth distributions in the sample have allowed the quantitative analysis of elemental composition and thickness of thin film on various substrates by EPMA, as shown in (Pouchou & Pichoir, 1991), and various software have been developed for the investigation of thin films based on the depth distribution function. An overview of the limitations to, improvements in, and new approaches to EPMA has been given (Llovet, Moy, Pinard, & Fournelle, 2021; Rinaldi & Llovet, 2015). However, this very useful technique to analyze thin films is underutilized likely due to the limited spread of information.

In the work described here, we characterized chromel and alumel alloys, both bulk and thin film, in order to assess the composition similarity of the deposited thin film to the bulk cathode, given the importance of these materials for their thermoelectric properties. The determination of the compositional similarity between the bulk cathode and the plasma condensed thin films is also of great importance regarding the wide application of FCVA technique. For this purpose, we first performed the techniques in their well-established protocols, namely quantitative SEM/EDS for the bulk and RBS analysis for the thin films. Then, we investigated the feasibility of compositional and thickness multi-element thin film analysis (chromel and alumel alloys) with thickness below 100 nm by quantitative SEM/EDS, adopting as reference the former RBS measurements of the thin films. In the studied cases, it was not possible to perform EDS analysis disregarding the substrate even at low beam acceleration voltage so that we evaluate different substrates (vitreous carbon, silicon, copper, and tin) so as to optimize the EDS compositional results. We used open-source software to analyze the data, namely GMRFilm (Waldo, Militello, & Gaarenstroom, 1993) and NIST DTSA-II (Ritchie, 2008). This article reports a case of thin film analysis (alumel) by RBS, which presented severely overlapping peaks. In this case, SEM/EDS analysis was crucial.

2 | MATERIALS AND METHODS

2.1 | Thin film deposition

Two sets of samples were produced, one set with deposited thin films of chromel alloy cathode (bulk nominal composition Cr 10 wt%, Ni 90 wt%, and bulk nominal density $\rho_{Chr} = 8.73\ g/cm^3$), and the other set with deposited thin films of alumel alloy cathode (bulk nominal composition Al 1.2 wt%, Si 1.6 wt%, Mn 1.8 wt%, Ni 95.4 wt%, and bulk nominal density $\rho_{Alm} = 8.60\ g/cm^3$). Film deposition was performed by FCVA on unbiased substrates, with base pressure of the system $P_b < 8 \times 10^{-6}$ Torr (before arc discharge), dc arc current ranging from 180 to 190 A, pulse length of 5 ms at a frequency of 1 Hz. The substrates were positioned at 7 cm from the end of the particle filter (more information about the substrates are given in the next section). The deposited films were of thickness less than 100 nm.

2.2 | Quantitative SEM/EDS analysis

The SEM/EDS technique (Goldstein et al., 2003; Heinrich, 1991; Lavrent'Ev, Korolyuk, & Usova, 2004) is rendered quantitative by the use of standards (substances of known composition and homogeneity over the beam interaction volume). Spectra of the standard and sample are acquired to obtain the value $k = \frac{I_i}{I_i}$, which relates the intensity of the element *i* obtained in the sample spectrum I_i to the intensity of the respective standard spectrum I_i, after subtraction of background radiation (Brehmsstrahlung). Application of some corrections is needed due to differences in electron backscattering, density, X-ray cross-section, energy loss, and absorption inside the solid. Many of these effects are dependent on atomic species involved. From the

mixture of elements arises the difference in elastic and inelastic scattering processes and the propagation of X-rays through the sample until reaching the detector.

There are different ways to approach the corrections. In the work described here, we used PAP model (Pouchou & Pichoir, 1991). This method is especially important because it allows the quantitative analysis of thin film (of the mass thickness μ_t) on substrates. SEM/EDS analysis was performed using a JEOL JSM6460 LV/Thermo Scientific NORAN System Six with nominal resolution 132 eV. Spectra were obtained using magnification of ×10,000 (area 10.2 × 12.7 μm^2) and take-off angle $\Psi = 40^\circ$ (to maximize the count rate by decreasing X-ray sample absorption, the choice of a range between 35° and 40° is common; Goldstein et al., 2017). The beam current, measured by a Faraday cup, was kept constant throughout acquisition of the spectra of the standards and the samples. Spectra of pure element standards were acquired, specifically nickel (Ni), manganese (Mn), chromium (Cr), silicon (Si), and aluminum (Al) (Structure Probe, Inc.; https://www.2spi.com/). The spectra were analyzed by NIST DTSA-II software for the purpose to obtain the k values (Goldstein et al., 2017, pp. 235–264) considering the characteristic X-ray K_α lines for each element and using Mn standard spectra for energy calibration of the detector (Fiori, Newbury, & Myklebust, 1981). The beam acceleration voltage E_0 was chosen to analyze the characteristic X-ray K_α lines, especially considering the major constituent of the alloys, namely nickel (Ni), which has a X-ray absorption edge energy $E_c^k = 8.3$ keV. The K lines have higher fluorescence yield and generally, less line overlaps. We also consider that the roughness requirement is less stringent for lines with higher energies than 1 keV, requiring roughness peak to peak less than 100 nm.

In order to have a suitable fluorescence yield but also to minimize the absorption effect, the spectra were obtained using a progression of beam acceleration voltages of 11, 15, and 20 keV. It is worth mentioning that a previous analysis was performed with $E_0 =$ 5 keV. The analysis with low acceleration voltages is a strategy used to convert the thin film analysis into a bulk case ("back-to-bulk-analysis"). Nevertheless, it was not possible to disregard the contribution of the substrate and the analytical totals (sum of concentrations of all elements accounted for analysis) were inadequate (less than 92%), suggesting inaccuracy of the measurements at beam acceleration voltage of 5 keV.

Since the electron beam interaction with the substrate is not at all negligible for the thin film case, we used a number of different substrates for the SEM/EDS analyses. The strategy of investigating a progression of atomic numbers for the substrates was similar to the application of beam acceleration voltages: to verify the accuracy of the results obtained for each condition, based on the elemental composition and thickness measurements obtained by RBS. Each substrate consisted of a single pure element selected considering its atomic number. Taking into account the nominal average atomic number for chromel ($\bar{Z}_{Chr} = 27.6$ and alumel ($\bar{Z}_{Alm} = 27.1$), we used different substrates with lower, similar and higher atomic numbers compared to $\bar{Z}_{Chr}$ and $\bar{Z}_{Alm}$. Thus, the substrates chosen were carbon ($Z = 6$), silicon ($Z = 14$), copper ($Z = 29$), and tin ($Z = 50$), all with purity greater than 99.9% (Alfa Aesar, https://www.alfa.com/; Silicon Sense, Inc., http://siliconsense.com/). Silicon was not used as a substrate for alumel since the alumel alloy itself contains silicon. Substrate polishing procedures were performed to obtain a peak-to-peak roughness[1] less than 100 nm (Tables 1 and 2) (Goldstein et al., 2003; Mayer, 2002) as measured by atomic force microscopy (AFM) (we used a Digital Instruments Nanoscope IIIA). EDS analysis of the substrates were performed to ensure the absence of contaminants due to polishing procedures.

We used the GMRFilm software (Waldo, 1995) which uses the $\varphi(\rho z)$ function[2] given by PAP model (Pouchou & Pichoir, 1991) to obtain the elemental thin film composition and thickness. The GMRFilm input data are basically the beam acceleration voltage, take-off angle Ψ (angle between the detector axis and the sample surface), and the $k_{element}$ of each constituent element (calculated by NIST DTSA-II) of each layer. The output data are composition (in wt%) and mass thickness (in units μg/cm^2). The thickness was calculated using the nominal density of each element weighted by its fractional content in the film.

We used Casino v.2 free software (Drouin et al., 2007), which uses a Monte Carlo (MC) method. The input data are the energy and number of simulated electron trajectories, take-off angle Ψ, and the composition and thickness of the sample layers including the substrate. From the input parameters, the k value is obtained using a simulated $\varphi(\rho z)$ function for each sample and standard (Kyser & Murata, 1974). The simulations were performed using nominal composition and nominal density and thickness as obtained by RBS.

TABLE 1 Roughness peak-to-peak of the substrates used for chromel thin film deposition for analyses performed by RBS and EDS techniques

Used for (technique)	Substrate	Roughness peak-to-peak (nm)
RBS	Carbon	35.7
EDS	Carbon	56.9
EDS	Copper	59.7
EDS	Tin	79.8

Note: Measurements performed by AFM with scan size of 15 μm.

TABLE 2 Roughness peak-to-peak of the substrates used for alumel thin film deposition for analyses performed by RBS and EDS techniques

Used for (technique)	Substrate	Roughness peak-to-peak (nm)
RBS	Carbon	38.3
EDS	Carbon	35.0
EDS	Copper	60.5
EDS	Tin	96.1

Note: Measurements performed by AFM with scan size of 15 μm.

2.3 | RBS analysis

RBS analysis was performed using a Tandetron Accelerator (LII-IF UFRGS, Porto Alegre, RS, Brazil), with a He++ ion beam, 16.5 keV resolution (FWHM), and detector positioned at a scattering angle of 165°. The measurements were performed at a beam energy of 1.50 and 3.00 MeV. The open-source software RUMP (Thompson, 1996) was used for analysis of the spectra.

3 | RESULTS AND DISCUSSION

In this section RBS spectra for chromel and alumel thin films (section 3.1) is shown; the composition and thickness data by quantitative SEM/EDS analysis for chromel and alumel thin films was compared to RBS data in order to evaluate the feasibility of this approach (section 3.2). In addition, the data comparison between bulk and thin film was performed to assess the composition similarity between the deposited thin film and the cathode used for deposition (section 3.3).

3.1 | RBS analysis

Figure 1 presents the spectra obtained by RBS of chromel and alumel thin films on vitreous carbon substrate and only the substrate, performed at 1.50 MeV, showing the spectrum region corresponding to the signal elements Ni, Mn, and Cr and Si and Al. In the figure is observed the overlap of Al peak and Si peak as well as Ni and Mn of the alumel thin film measurement and the overlap of Ni and Cr of the chromel thin film measurement.

In the measurements performed at 3.00 MeV (Figure 2) was possible to resolve the overlapping peaks of the Ni and Cr. However, the overlap for Ni and Mn as well as Al and Si peaks of the alumel thin film measurement was unable to resolve even at higher energy.

The RBS results for both chromel and alumel alloys show overlapping peaks, which complicates the interpretation for quantification of individual constituent elements. For the chromel films, the peaks can be resolved and we quantified the Ni and Cr using a beam energy of 3.00 MeV. However, for the alumel films, the severely overlapping peaks for Ni and Mn, as well as for Al and Si, made resolution not possible. Thus, the quantification by EDS was crucial. The RBS results are presented in the next section.

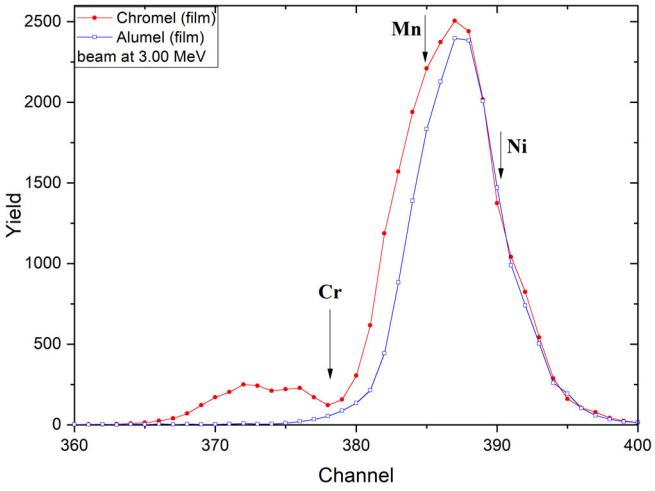

FIGURE 2 RBS spectra of chromel and alumel thin films. Measurements performed with He++ beam at 3.00 MeV

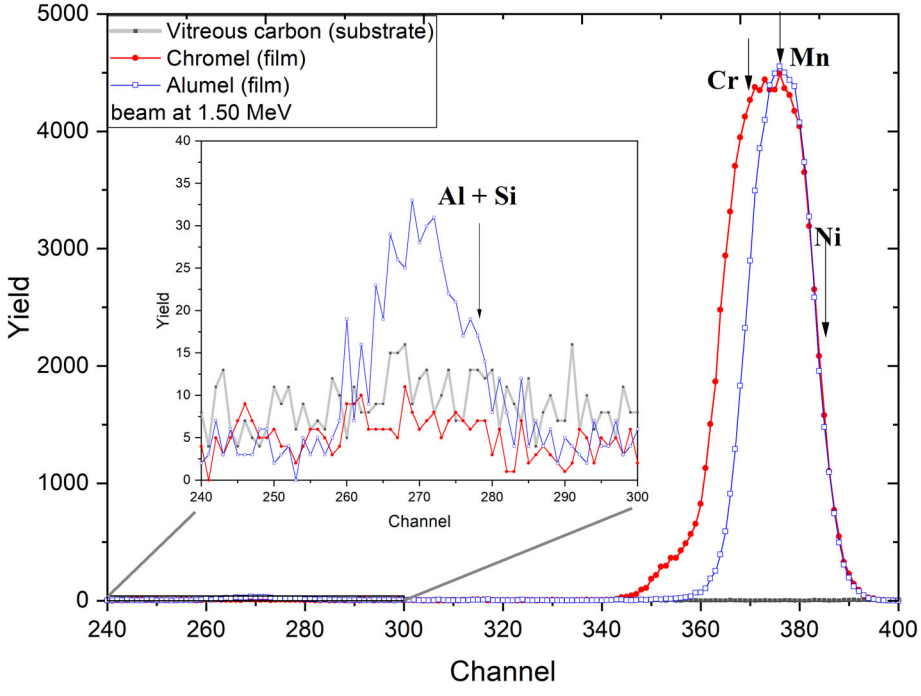

FIGURE 1 RBS spectra of chromel and alumel thin films and vitreous carbon substrate. Measurements performed with He++ beam at 1.50 MeV

3.2 | Feasibility of thin film analysis by quantitative SEM/EDS

As already mentioned, it was not possible to use the strategy to convert the thin film into a bulk case performing the analysis at acceleration voltages, therefore not being able to neglect the substrate. To clarify why it may be difficult to assess thin film composition and thickness by SEM/EDS, taking into consideration the electron beam energy range typically used in this technique, we show results of Monte Carlo simulations of the beam interaction with the sample as an example, performed using the Casino v.2 program (Drouin et al., 2007) (Figure 3). The figure shows trajectories of primary

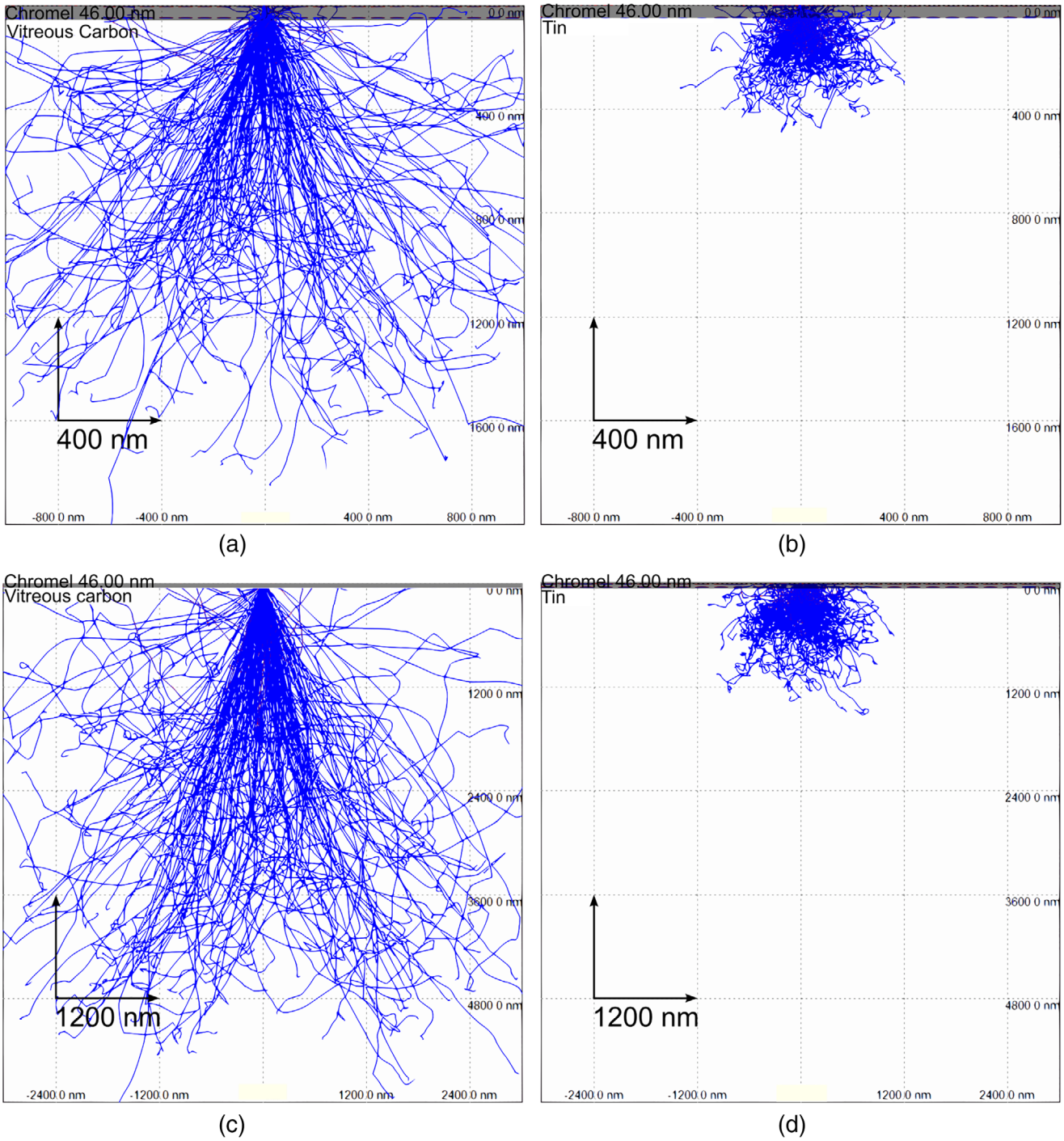

FIGURE 3 Monte Carlo simulations of the interaction of the primary electron beam with the sample; we used the Casino v2.48 program (Drouin et al., 2007). The simulation shows the trajectory of primary electrons in a chromel layer of thickness of 46.0 nm on C and Sn substrates, for beam energies of 11 and 20 keV. (a) Chromel on C substrate at 11 kV. (b) Chromel on Sn substrate at 11 kV. (c) Chromel on C substrate at 20 kV. (d) Chromel on Sn substrate at 20 kV

electrons, for a 46.0 nm film of chromel on C ($Z = 6$) and on Sn ($Z = 50$) substrate at 11 and 20 kV.

From these simulations (Figure 3), we can semiquantitatively estimate the thickness of the interaction volume. Figure 3b shows the simulation for a chromel film on a tin substrate (higher atomic number, $Z = 50$) and a beam energy of 11 keV; we see that in this case the film represents about 10% of the interaction volume. With the same film on a C substrate (Figure 3a) (lower atomic number, $Z = 6$) the film represents less than 3% of the interaction volume. At 20 kV (Figure 3c,d), the chromel film represents about 1 and 4% of the interaction volume, respectively. Thus, we can very clearly see why it could be inadequate using the SEM/EDS technique to assess thin film composition and thickness.

In Figure 4, we presented an example of experimentally determined and simulated k values as a function of beam energy for each element on various substrates. (All experimental values are listed in Tables S1 and S2, Supporting Information). As can be seen from the simulations, the k values of the thin film elements change with beam energy, as expected. This happens primarily because of the inhomogeneity within the beam–sample interaction volume. The interaction volume increases with beam energy, and thus the k values decrease with increasing beam energy because the film becomes a smaller fraction of the interaction volume.

The variation of k values of the thin film elements on different substrates is due to the change in electron backscattering. A substrate with higher atomic number provides greater scattering, increasing the signal coming from the film. The reverse is true for lighter element substrates. This behavior can be seen in Figure 4. It can be observed that the k for carbon substrate presented better agreement between the experimental and simulated value despite the fact that the film signal represents a range between 4 and 1% of the beam interaction volume as previously seen. It also can be observed that the agreement between simulated and experimental all values improve with increasing beam energy. In general, the simulated values were overestimated concerning the experimental data, mainly at low beam energy. (Statham, Llovet, & Duncumb, 2012) reports systematic behavior of Monte Carlo

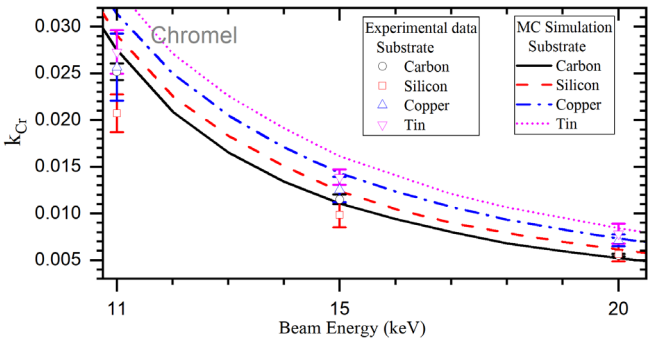

FIGURE 4 Experimental and simulated k values of the element Cr for chromel film as a function of beam energy. The simulation was performed for a chromel film of 46.0 nm thickness (RBS result) and nominal bulk composition, on four different substrates (C, Si, Cu, and Sn), beam at normal incidence of 20,000 electrons and take-off angle $\Psi = 40°$

TABLE 3 Elemental composition and thickness t for chromel thin films on different substrates as determined by quantitative EDS analysis, measured at 11, 15, and 20 keV

		Concentration (wt%)		
Z_{Subs}	E_0 (keV)	Ni	Cr	t (nm)
6	11	91.1 ± 0.5	9.0 ± 0.5	50.4 ± 1.4
	15	89.7 ± 0.6	10.3 ± 0.6	46.0 ± 1.5
	20	90.7 ± 0.4	9.3 ± 0.3	49.7 ± 1.1
14	11	91.2 ± 0.9	8.8 ± 0.9	40.5 ± 1.9
	15	90.1 ± 0.9	9.9 ± 0.9	37.9 ± 2.4
	20	90.3 ± 1.4	9.7 ± 1.4	38.7 ± 1.4
29	11	90.3 ± 1.1	9.7 ± 1.1	41.1 ± 2.7
	15	89.5 ± 1.1	10.5 ± 1.1	38.1 ± 1.5
	20	90.4 ± 0.6	9.6 ± 0.6	43.3 ± 2.4
50	11	66 ± 12	34 ± 12	14 ± 5
	15	66 ± 13	34 ± 13	15 ± 5
	20	57 ± 8	43 ± 8	11.4 ± 2.4

simulations, which overestimate k values with the increasing of the experimental values (for low thickness) as observed here. However, this trend occurs at much higher values of experimental k values.

Table 3 lists the experimental results for elemental composition and thickness for chromel thin films on substrates having different atomic number Z_{Subs}, obtained as described above in section 2.2. Table 4 lists similarly for alumel thin films.

To evaluate the thin film composition and thickness analysis by quantitative SEM/EDS, we compared the results with RBS measurements. Tables 5 and 6 show the elemental concentration results obtained by EDS and RBS techniques. Student's t-Test is used for comparison. The EDS values correspond to the mean weighting by inverse variance of values obtained at 11, 15, and 20 kV. Note that the values obtained by RBS analysis for the alumel thin film are the sum of the concentrations of the Ni and Mn (Ni + Mn) and Al and Si (Al + Si) due to overlapping peaks as previously discussed in section 3.1. Statistical criteria were used to compare the values shown in Tables 5 and 6. The rejection or nonrejection of the means equality hypothesis (null hypothesis) was based on the p value (Levine, Stephan, & Szabat, 2008), since the p value reflects the probability of observing the same result or more extreme assuming that the null hypothesis is true. Thus, here we infer compatibility between the means if p value $\geq \alpha$, and we adopt a significance level $\alpha = .05$ (5%).

We found that Cu substrates ($Z = 29$) used for the EDS analysis yield results that are compatible with the RBS composition measurements, for all elemental constituents of both chromel and alumel films. The Si ($Z = 14$) substrate used in the chromel analysis also showed compatibility between the EDS and RBS results. However, the quantitative analyses by EDS and RBS were not compatible for C ($Z = 6$) and Sn ($Z = 50$) substrates. Of the different substrates used for chromel and alumel film depositions, Cu ($Z = 29$) has atomic number closest to

TABLE 4 Elemental concentration and thickness *t* for alumel thin films on different substrates as determined by quantitative EDS analysis, measured at 11, 15, and 20 keV

		Concentration (wt%)				
Z_{Subs}	E_0 (keV)	Ni	Mn	Si	Al	*t* (nm)
6	11	94.9 ± 1.4	3.1 ± 0.9	0.9 ± 0.2	1.0 ± 0.3	26.1 ± 1.8
	15	94.1 ± 1.1	3.4 ± 0.9	1.2 ± 0.3	1.3 ± 0.5	26.1 ± 0.7
	20	95.2 ± 1.1	2.4 ± 1.0	1.1 ± 0.6	1.3 ± 0.3	27.8 ± 1.7
9	11	95.9 ± 0.6	2.5 ± 0.5	0.7 ± 0.2	0.9 ± 0.1	33 ± 4
	15	94.6 ± 0.9	3.0 ± 0.9	1.0 ± 0.5	1.5 ± 0.2	34 ± 3
	20	93.8 ± 1.0	3.5 ± 1.0	0.9 ± 0.4	1.7 ± 0.3	38.5 ± 2.5
0	11	94.4 ± 0.6	3.0 ± 0.5	1.5 ± 0.2	1.2 ± 0.1	30 ± 3
	15	92.9 ± 1.6	3.0 ± 1.3	2.5 ± 0.3	1.6 ± 0.3	30.4 ± 1.9
	20	91.9 ± 0.7	2.0 ± 0.5	3.6 ± 0.3	2.5 ± 0.3	35.5 ± 1.6

TABLE 5 Comparison by *t*-Test of the elemental composition and thickness *t* for chromel thin films by quantitative EDS and RBS analysis

	Substrate	Concentration (wt%)		
	Z	Ni	Cr	*t* (nm)
EDS	6	90.6 ± 0.3	9.39 ± 0.24	49.0 ± 0.7
	14	90.6 ± 0.6	9.4 ± 0.6	39.1 ± 1.0
	29	90.2 ± 0.5	9.8 ± 0.5	39.8 ± 1.2
	50	61 ± 6	39 ± 6	12.3 ± 2.0
RBS	–	Ni	Cr	*t* (nm)
		90 ± 6	10.3 ± 0.7	46 ± 5
t-Test *p* value	*Z* (EDS)	Ni	Cr	*t* (nm)
	6	.03*	.022*	.020*
	14	.12	.12	.007*
	29	.20	.20	.011*
	50	.015*	.015*	.0012*

Note: *Statistically significant result (p value < α).

that of both the chromel alloy ($\bar{Z}_{Chr} = 27.6$) and the alumel alloy ($\bar{Z}_{Alm} = 27.1$). Llovet and Merlet (2010) have reported that most programs for EDS thin film analysis assume that they are bulk samples, described by the mean of the same mathematical parameters, an assumption that should be acceptable when the scattering and energy loss of electrons (i.e., the atomic number *Z*) in film and substrate are similar. Thus the fact that here the Cu substrate yields the best results is likely due to the good match between *Z* for the film and *Z* for the substrate.

Concerning the thickness, the alumel thin film sample on Cu substrate (Table 6), as analyzed by quantitative EDS, is consistent with the RBS results. Although we have found only one thickness result of our two test cases compatible with RBS, at a significance level $\alpha = .05$, we can nevertheless obtain a good approximation of film thickness by using a substrate of similar atomic number.

3.3 | Comparison between bulk and thin film

As seen in the previous section, quantitative SEM/EDS analysis was able to assess the thin film composition of the chromel and alumel using a substrate of similar atomic number (copper for both), quantifying each alloy constituent element. It is worth mentioning that if we only had RBS results, it would not be possible to compare each element due to severely overlapping peaks. Thus, we used the EDS results to verify the composition similarity between thin film deposited and material bulk used to.

Tables 7 and 8 show a comparison of the elemental concentrations as determined by quantitative EDS of the cathode material (bulk) and of the thin film deposited by FCVA. The thin film EDS values that were taken for comparison refer to the copper substrate samples.

TABLE 6 Comparison by *t*-Test of the elemental composition and thickness *t* for alumel thin films by quantitative EDS and RBS analysis

	Substrate	Concentration (wt%)				
	Z	Ni	Mn	Si	Al	*t* (nm)
EDS	6	94.7 ± 0.7	3.0 ± 0.5	1.00 ± 0.16	1.17 ± 0.20	26.3 ± 0.6
	29	95.2 ± 0.4	2.8 ± 0.4	0.77 ± 0.17	1.08 ± 0.09	36.0 ± 1.8
	50	93.3 ± 0.4	2.5 ± 0.3	2.23 ± 0.15	1.35 ± 0.09	32.9 ± 1.2
RBS	–	Ni + Mn		Si + Al		*t* (nm)
		99 ± 7		1.40 ± 0.07		39 ± 4
t-Test *p* value	*Z* (EDS)	Ni + Mn		Si + Al		*t*
	6	.22		.03*		.0008*
	29	.19		.05		.13
	50	.013*		.0020*		.014*

Note: *Statistically significant result (p value < α).

TABLE 7 Comparison by *t*Test of chromel elemental (Ni and Cr) concentration in the bulk cathode material and in the thin film deposited by FCVA, as determined by quantitative EDS

Chromel			
Element	**Bulk**	**Thin film**	***t*-Test *p* value**
Ni	90.3 ± 0.5	90.2 ± 0.5	.9
Cr	9.72 ± 0.19	9.8 ± 0.5	.8

TABLE 8 Comparison by *t* test of alumel elemental (Ni, Mn, Si, Al) concentration in the bulk cathode material and in the thin film deposited by FCVA, as determined by quantitative EDS

Alumel			
Element	**Bulk**	**Thin film**	***t*-Test *p* value**
Ni	95.1 ± 0.8	95.2 ± 0.4	1.0
Mn	2.02 ± 0.14	2.8 ± 0.4	.09
Si	1.65 ± 0.04	0.77 ± 0.17	.013*
Al	1.15 ± 0.05	1.08 ± 0.09	.27

Note: *Statistically significant result (*p* value < α).

The elemental concentrations of the bulk and thin film materials of the same alloy—chromel—show no statistical significant difference, taking a significance level of $\alpha = .05$, as is evident from Table 7. For the alumel thin film, the concentration of silicon shows a significant difference from the bulk, considering $\alpha = .05$, as shown in Table 8. Thus, these values are incompatible, implying that alumel thin film deposition by FCVA results in a different composition in the film than in the cathode, specifically for Si.

It has been reported (Anders, 2008; Brown, 1998) that the elemental concentration of thin films deposited by FCVA reflects the composition of the cathode material, although small deviations were found. However, a significant difference between the composition of the cathode material and the plasma formed from it has been reported (Sasaki & Brown, 1989) for the case of nonmetallic components, which is consistent with our results.

4 | CONCLUSIONS

We have demonstrated in detail the application of quantitative EDS for the determination of composition and thickness of chromel and alumel alloys. Recognizing that RBS is the most widely used technique for determination of elemental composition and mass thickness of thin films, we have shown that quantitative EDS provides an alternative approach that can be advantageous via its capability of quantifying these characteristics in both thin film and bulk material. We have shown that chromel thin films deposited by FCVA have elemental compositions that are in good concurrence with that of the cathode material used for their FCVA deposition. However, some significant differences were found for alumel thin films, probably due to the presence of the nonmetallic element silicon.

The elemental composition of chromel and alumel thin films as determined by RBS and by EDS (with Cu substrates) was in good agreement. We find that use of a substrate material with atomic number close to the mean atomic number of the film constituent materials proved to be relevant for reliable EDS results, when compared to RBS. This may be due to the fact that the correction by atomic number for Cu substrates is lower, since it was the substrate with the atomic number closest to the average atomic numbers of the chromel and alumel alloys. For alumel thin films, there was severe overlapping of peaks in the RBS spectra that could not be resolved, and thus EDS was crucial. Film thickness estimates as determined by EDS and by RBS were found to be in good agreement only for the alumel thin films, but nevertheless the difference between the two estimates (from EDS and from RBS) for chromel thin film was less than 15% (with Cu substrate). We conclude that it is indeed feasible to obtain a reasonable estimate of the thin film thickness using the quantitative EDS technique as described. Another approach that can be considered for obtaining the elementary concentrations of thin films by quantitative EDS can be through adjustment between experimental and theoretical curves of *k* values as a function of the beam acceleration voltages E_0. This approach can produce more accurate results compared to those that result from analysis on a specific E_0 or an average of specific E_0 (the latter approach was applied in the work described here). There are currently programs that are used

for this purpose, such as STRATAGEM (http://www.samx.com/index.html.en) or X-FILM (Llovet & Merlet, 2010), but they are not free software.

ACKNOWLEDGMENTS

This work was supported by the São Paulo Research Foundation (FAPESP, Brazil) under grant number 2000/08231-1, was financed in part by the Coordenação de Aperfeiçoamento de Pessoal de Nível Superior (CAPES, Brazil – Finance Code 001) and by Conselho Nacional de Desenvolvimento Científico e Tecnológico (CNPq, Brazil) under grant number 156484/2014-5. We are grateful to workers at the Laboratório de Filmes Finos of the Institute of Physics, University of São Paulo (LFF – IF USP) for support throughout the experiments. We also thank the Laboratório de Implantação Iônica of the Institute of Physics, Federal University of Rio Grande do Sul (LII – IF UFRGS), for the RBS analysis.

CONFLICT OF INTEREST

The authors declare no potential conflict of interest.

ENDNOTES

[1]The roughness peak-to-peak of the silicon substrate was not measured due to high level of polishing (roughness RMS < 1 nm).

[2]$\varphi(\rho z)$ is a function that describes the X-ray excitation variation over the mass depth ρz (surface layer density of the substance from the surface to the depth z) of the target, proposed by Castaing (1951).

DATA AVAILABILITY STATEMENT

The data that support the findings of this study are available in the supplementary material of this manuscript.

ORCID

Raissa Lima de Oblitas https://orcid.org/0000-0002-2997-4103
Fernanda de Sá Teixeira https://orcid.org/0000-0002-8986-3210
Maria Cecília Salvadori https://orcid.org/0000-0002-2372-1746

REFERENCES

Anders, A. (2008). *Cathodic arcs*. Springer series on atomic, optical, and plasma physics (Vol. 50). New York, NY: Springer. https://doi.org/10.1007/978-0-387-79108-1

Brown, I. G. (1998). Cathodic arc deposition of films. *Annual Review of Materials Science*, *28*, 243–269. https://doi.org/10.1146/annurev.matsci.28.1.243

Castaing, R. (1951). Application of electron probes to local chemical and crystallographic analysis. University of Paris. Available online (translation): https://the-mas.org/castaings-famous-1951-thesis/

Drouin, D., Couture, A. R., Joly, D., Tastet, X., Aimez, V., & Gauvin, R. (2007). CASINO V2.42: A fast and easy-to-use modeling tool for scanning electron microscopy and microanalysis users. *Scanning*, *29*, 92–101.

Fiori, C. E., Newbury, D. E., & Myklebust, R. L. (1981). *Artifacts observed in energy dispersive X-ray spectrometry in electron beam instruments—A cautionary guide* (NIST Special Publication 604). Washington, DC: US Government Printing Office.

Goldstein, J., Newbury, D. E., Echlin, P., Joy, D. C., Romig, A. D., Jr., Lyman, C. E., … Lifshin, E. (2003). *Scanning electron microscopy and X-ray microanalysis*. New York, NY: Kluwer Academic/Plenum.

Goldstein, J. I., Newbury, D. E., Michael, J. R., Ritchie, N. W. M., Scott, J. H. J., & Joy, D. C. (2017). *Scanning electron microscopy and X-ray microanalysis*. New York, NY: Springer.

Heinrich, K. F. J. (1991). Strategies of electron probe data reduction. In *Electron probe quantitation* (pp. 9–18). New York, NY: Springer Science & Business Media.

Kang, K. W., Limandri, S., Castellano, G., Suárez, S., & Trincavelli, J. (2017). Thickness determination of anodic titanium oxide films by electron probe microanalysis. *Materials Characterization*, *130*, 50–55.

Kyser, D. F., & Murata, K. (1974). Quantitative electron microprobe analysis of thin films on substrates. *IBM Journal of Research and Development*, *18*, 352–363.

Lavrent'Ev, Y. G., Korolyuk, V. N., & Usova, L. V. (2004). Second generation of correction methods in electron probe X-ray microanalysis: Approximation models for emission depth distribution functions. *Journal of Analytical Chemistry*, *59*, 600–616.

Levine, D. M., Stephan, D. F., & Szabat, K. A. (2008). *Statistics for managers using Microsoft Excel*. London, England: Pearson Education Limited.

Liu, Y., Mitsutake, Y., & Monde, M. (2020). Development of fast response heat transfer measurement technique with thin-film thermocouples. *International Journal of Heat and Mass Transfer*, *162*, 120331.

Llovet, X., & Merlet, C. (2010). Electron probe microanalysis of thin films and multilayers using the computer program XFILM. *Microscopy and Microanalysis*, *16*, 21–32.

Llovet, X., Moy, A., Pinard, P. T., & Fournelle, J. H. (2021). Electron probe microanalysis: A review of recent developments and applications in materials science and engineering. *Progress in Materials Science*, *116*, 100673.

Martins, D. R., Salvadori, M. C., Verdonck, P., & Brown, I. G. (2002). Contamination due to memory effects in filtered vacuum arc plasma deposition systems. *Applied Physics Letters*, *81*, 1969–1971.

Mayer, M. (2002). Ion beam analysis of rough thin films. *Nuclear Instruments & Methods in Physics Research. Section B, Beam Interactions with Materials and Atoms*, *194*, 177–186.

Pouchou, J.-L., & Pichoir, F. (1991). Quantitative analysis of homogeneous or stratified microvolumes applying the model "PAP". In K. F. J. Heinrich & D. E. Newbury (Eds.), *Electron probe quantitation* (pp. 31–75). New York, NY: Plenum Press. https://doi.org/10.1007/978-1-4899-2617-3_4

Rinaldi, R., & Llovet, X. (2015). Electron probe microanalysis: A review of the past, present, and future. *Microscopy and Microanalysis*, *21*, 1053–1069.

Ritchie, N. W. M. (2008). *NIST DTSA-II*. Retrieved from https://www.cstl.nist.gov/div837/837.02/epq/dtsa2/

Sasaki, J., & Brown, I. G. (1989). Ion spectra of vacuum arc plasma with compound and alloy cathodes. *Journal of Applied Physics*, *66*, 5198–5203.

Satish, T. N., Rakesh, K. P., Uma, G., Umapathy, M., Chandrasekhar, U., Rao, A. N. V., & Petley, V. (2017). Functional validation of K-type (NiCr-NiMn) thin film thermocouple on low pressure turbine nozzle guide vane (LPT NGV) of gas turbine engine. *Experimental Techniques*, *41*, 131–138. https://doi.org/10.1007/s40799-016-0162-1

Statham, P., Llovet, X., & Duncumb, P. (2012). Systematic discrepancies in Monte Carlo predictions of k-ratios emitted from thin films on substrates. *IOP Conference Series: Materials Science and Engineering*, *32*, 012024.

Thompson, M. O. (1996). *RUMP*. Retrieved from http://www.genplot.com/doc/rump.htm.

Waldo, R. A. (1995). *GMR film*. Retrieved from http://www.amc.anl.gov/anlsoftwarelibrary/02-MMSLib/XEDS/GMRFILM/

Waldo, R. A., Militello, M. C., & Gaarenstroom, S. W. (1993). Quantitative thin-film analysis with an energy-dispersive x-ray detector. *Surface and Interface Analysis*, *20*, 111–114. https://doi.org/10.1002/sia.740200204

Walkowicz, J., Bujak, J., & Zavaleyev, V. (2010). The effect of unintentional oxygen incorporation into Cr-CrN-DLC coatings deposited by MEPIIID method using filtered Cathodic vacuum arc carbon and metal plasma. *Problems of Atomic Science and Technology*, *6*, 179–181.

SUPPORTING INFORMATION

Additional supporting information may be found in the online version of the article at the publisher's website.

How to cite this article: Lima de Oblitas, R., de Sá Teixeira, F., & Salvadori, M. C. (2021). Determination of the composition and thickness of chromel and alumel thin films on different substrates by quantitative energy dispersive spectroscopy analysis. *Microscopy Research and Technique*, 1–10. https://doi.org/10.1002/jemt.23917